



Cite this: *RSC Sustainability*, 2024, **2**, 3362

## Sustainable micro-cellulosic additives for high-density fiber cement: emphasis on rheo-mechanical properties and cost–performance analysis†

Sreenath Raghunath, <sup>ab</sup> Mahfuzul Hoque, <sup>ab</sup> Behzad Zakani, <sup>ab</sup> Akash Madhav Gondaliya <sup>ab</sup> and E. Johan Foster <sup>\*ab</sup>

To combat climate change (*i.e.*, global warming), reducing the CO<sub>2</sub> footprint of cement-based building materials can be substantiated by incorporating cellulosic fibers into the cement matrix (fiber cement). However, such materials design imposes tremendous technical challenges towards the fabrication process, interlinked to its rheo-mechanical properties. Thus, polycarboxylate-based (petrochemical-derived) rheology modifiers and silica-based (carcinogenic) additives are usually added to the fiber-cement slurry. Micro-cellulosic biomaterials are technically a viable eco-friendly alternative, capable of modifying the rheo-mechanical properties, yet to be explored for high-density (>8 wt% fiber) fiber cement. Herein, we have employed morphologically distinctive alpha-cellulose (AC) and microcrystalline cellulose (MCC) as rheo-mechanical additives. The total content of biomaterials in the fiber cement was up to 12 wt%, where the ratio between the micro-cellulosic additive (AC/MCC) and the cellulosic fibers varied proportionally. As a result, various composites were fabricated based on combinations 1 (AC and fibers) and 2 (MCC and fibers), and their rheo-mechanical properties were characterized to understand the effect of this morphologically distinctive micro-cellulose. Firstly, the rheological analysis revealed that combination 1 reduced the yield stress (improving the workability) at any content – with 4 wt% AC content indicating a maximum reduction in yield stress of 30%. Secondly, flexural strength analysis revealed that combinations 1 and 2 improve the modulus of rupture (MOR), and combination 2 (at 6 wt% MCC content) resulted in a 42% increase in MOR. Finally, we presented the cost-to-performance ratio analysis (economic perspective), highlighting the positive ramifications of this sustainable rheology modifier and additives for the cement-based composite – an avenue for low-embodied carbon building materials without compromising the strength-to-weight ratio.

Received 5th June 2024  
Accepted 5th September 2024

DOI: 10.1039/d4su00287c  
[rsc.li/rscsus](http://rsc.li/rscsus)



### Sustainability spotlight

The research presented in this paper advances sustainability by developing eco-friendly high-density fiber cement composites using micro-cellulosic biomaterials, specifically alpha-cellulose (AC) and microcrystalline cellulose (MCC). This innovation reduces the reliance on carbon-intensive petrochemical-based rheology modifiers and silica-based additives, significantly lowering the CO<sub>2</sub> footprint of building materials. The enhanced rheo-mechanical properties and cost–performance ratio align with the United Nations Sustainable Development Goals (SDGs), particularly SDG 12: responsible consumption and production. This study paves the way for the production of sustainable, low-carbon building materials, contributing to global efforts to mitigate climate change and promote sustainable construction practices.

## 1 Introduction

The reduction of carbon dioxide (CO<sub>2</sub>) emissions from materials like cement is crucial to mitigating global warming since it

is responsible for 8% of global CO<sub>2</sub> emissions. One of the ways to curb cement's impact on climate change is to reduce its content in a range of building materials, *e.g.*, reinforced cement (fiber cement). Importantly, it could potentially be a key driver in attaining the sustainable development goals laid out by the United Nations (especially SDG 12, which focuses on "ensuring responsible consumption and production practices").<sup>1</sup> In this regard, wood-derived pulp fibers (with or without lignin) have been prevalently used in composite (non-structural) engineering.<sup>2</sup> However, its fabrication process suffers from poor rheology of the slurry (pre-production step) and mechanical

<sup>a</sup>Department of Chemical and Biological Engineering, The University of British Columbia, 2385 East Mall, Vancouver, V6T 1Z4, BC, Canada. E-mail: [johan.foster@ubc.ca](mailto:johan.foster@ubc.ca)

<sup>b</sup>Bioproducts Institute, 2385 East Mall, Vancouver, V6T 1Z4, BC, Canada

† Electronic supplementary information (ESI) available. See DOI: <https://doi.org/10.1039/d4su00287c>

(flexural) strength of the composite. To tackle these challenges, petrochemical-based superplasticizers as rheology modifiers and siliceous materials as additives (fillers) have been employed to attain favorable rheo-mechanical properties.<sup>3,4</sup>

Although natural fibers have a range of physical attributes, *i.e.*, high aspect ratio, these mechanically strong fibers inadvertently render poor dispersion (inconsistent fiber cement slurry), a bottleneck in increasing the fiber content in the composite. To a degree, this is resolved through viscosity-modifying admixtures (VMA), also known as superplasticizers. These water-soluble admixtures (semi-synthetic and synthetic) positively alter the rheological behavior while affecting the other facets of processing, *e.g.*, hydration and setting time and its physico-chemical properties (porosity and mechanical properties).<sup>5,6</sup> Over the years, a broad range of polymeric superplasticizers, *e.g.*, polycarboxylate-based (PCE) ones, have been developed, which exhibit balanced rheology, micro-mechanics, and hydraulic cement chemistries.<sup>7-9</sup> On the other hand, bio-based superplasticizers, *i.e.*, functionalized lignin<sup>10</sup> as well as starch sulphonate,<sup>11</sup> methylcellulose (derived from sugarcane bagasse),<sup>12</sup> and algal biomass,<sup>13,14</sup> have been reported to improve the workability of the (fiber) cement slurry. However, biopolymers/biomass slow down the hydration kinetics; for instance, polysaccharides (*e.g.*, starch) are well known for their utility as hardening retarders,<sup>15</sup> used in ready-mix concrete applications.

Another key component in cement-composite design is silica-based additives (*e.g.*, silica sand, silica fume, and silica flour), ubiquitous in the building materials industry, and capable of tuning the rheo-mechanical properties according to application needs.<sup>3,4</sup> However, owing to the growing health and environmental concerns related to the use and production of (crystalline) silica-based additives,<sup>16</sup> research on sustainable and user-benign additives has gained momentum in recent years.<sup>17,18</sup> In particular, cellulosic micro-particles are considered for low-carbon (structural) building materials, like development of microbially induced concrete owing to their abundance in natural plant and waste biomass.<sup>19</sup> In our earlier communication, we leveraged nanocrystalline cellulose (CNC) in fabricating fiber cement without any PCE (superplasticizer) and silica (additive). Interestingly, CNC as the sole biobased additive modified the slurry rheology, accelerated the hydration kinetics, and enhanced the mechanical properties of the composite.<sup>20,21</sup> However, at high content (*i.e.*, 4 wt%) of CNC, workability becomes poor, and the high raw materials cost (production cost ~USD 5900/t)<sup>22</sup> of nanomaterials imposes a significant barrier to commercial-scale adoption. Hence, exploration of cost-effective natural additives is crucial without negating the materialistic benefits of CNC.<sup>21</sup> To this end, exploring polysaccharides as a class of biomaterials could be of techno-economic interest for further research. Polysaccharides are predominantly viable, *e.g.* cellulose, which is the most abundant (accounting for 61.8% of all structural biobased polymers produced as of 2013)<sup>23</sup> biopolymer and can meet the requirements and supply-chain demands of the construction industry.<sup>24</sup>

Alpha-cellulose (AC) and microcrystalline cellulose (MCC) are two of the promising candidates in the polysaccharide class

of materials as they offer techno-economic advantages as compared to CNC while showing similar materials chemistry. The prevalent sources of AC are wood (40–50%) and cotton (90%), and it is often extracted (alkaline and bleaching treatment) from sources such as rice straw<sup>25</sup> and cocoa pod husk during the chemical pulping process.<sup>25,26</sup> On the other hand, to produce MCC, often AC extracted from wood/plant sources is used as a starting material. The purified cellulose is then subjected to a mild acid hydrolysis (*e.g.*, 2 M hydrochloric acid at 105 °C for 15 min), where the amorphous components in AC (though in minor proportions) are selectively hydrolyzed, resulting in the release of crystallites which are then mechanically dispersed in the solution before drying.<sup>27</sup> Regarding physico-chemical features, both of them are fibrous and exhibit similar chemical functionality. However, the chemical and physical treatment of natural materials strongly affects the size distribution and the degree of crystallinity of the processed cellulosic material. Thus, the key differences between the AC and MCC are size and the presence/absence of amorphous hemicellulose (non-crystalline, branched polymer with low molecular weight).

In the context of cement chemistries, note that the intrinsic high alkalinity (cement paste/pore solution has a pH range of ≈12–13)<sup>28</sup> of the cement-matrix raises additional challenges regarding the chemical stability of the biopolymers. As such, crystalline cellulosic materials would be suitable as compared to the amorphous cellulosic and lignocellulosic materials.<sup>29,30</sup> Upon surveying the literature, it was intriguing that the research about AC and MCC for low-carbon building materials is scarce. Note that the AC is yet to be reported as a rheology modifier and additive in reinforced cement composite. On the other hand, Gómez Hoyos *et al.* evaluated the effect of MCC on the hydration kinetics of cement paste.<sup>31</sup> Rocha Ferreira *et al.* revealed a reduction (15%) of the setting time after adding MCC in cement/geopolymer (inorganic polymeric material composed of 3D networks of aluminosilicates) systems (metakaolin-based). The compressive strength was improved, ~55% for the cement system and ~7% for the geopolymer system. It was hypothesized that the geopolymer matrix was more detrimental than the cement matrix for MCC. In other words, MCC contributed to the compressive strength despite the high alkalinity of cement paste, but under the harsher matrix conditions of the geopolymer, it was not able to due to chemical degradation (yet to be proven).<sup>32</sup>

Therefore, based on the current research gap, we have chosen AC and MCC as additives to develop high-density fiber cement devoid of traditional superplasticizers and silica-based (inert) fillers. By reducing any physico-chemical effect of the traditional carbon-intensive additives, we can ensure how these biomaterials can influence the rheo-mechanical properties of the composite (fiber cement). In this study, we varied the content (in wt%) between the AC (or MCC) and cellulosic fibers, denoted as NBSK, which stands for Northern Bleached Softwood Kraft pulp fibers. Based on the findings from our earlier work with CNC as a multifunctional (expensive) additive, we set 12 wt% as the baseline for total biomaterial content.

In this research, we have formulated the recipe in two combinations with NBSK fibers in terms of AC (combination 1)



and MCC (combination 2) as micro-cellulosic additives and performed in-depth rheo-mechanical analysis. However, in each formulation, the relative content (in wt%) between AC (or MCC) and NBSK was varied, and has not been reported to date for fiber cement, with one of the major application segments being the building (residential and non-residential) façade. Finally, we presented performance metrics data, *i.e.*, strength to weight (*S/W*) and cost to performance (*C/P*) analysis to bridge the gap between lab-based findings and commercially relevant requirements. We believe the research presented in this work will inspire the stakeholders to accelerate the adoption of biomaterials in next-generation cement admixture industries, which is crucial to improving the sustainability of the construction industry.

## 2 Materials and methodology

### 2.1 Raw materials

The matrix material, ordinary Portland cement (Type I), was procured from Lafarge Canada. The reinforcing fibers, northern bleached softwood Kraft pulp (denoted as NBSK), were obtained from Canfor, Canada. We gratefully acknowledge each provider for their kind contribution. Microcrystalline cellulose (MCC) (Avicel® PH-101) and alpha-cellulose (AC) were procured from Sigma-Aldrich, Canada. All these raw materials were used as received during composite fabrication. Reverse Osmosis (RO) water was used to mix the components to form a fiber-cement slurry. The bulk physico-chemical properties have been detailed in the ESI (Tables S1–S8†) to conserve space in the main manuscript.

### 2.2 Fabrication process of fiber cement: matrix development and optimization of the content limit for micro-cellulosic additives

Micro-cellulosic additives (AC and MCC) were premixed (duration: 2 minutes) with cement prior to the mixing with the refined NBSK fibers (see Fig. S1† for refined fiber properties). The rest of the steps are mentioned in our previous work (see the experimental section in ref. 21 for details).<sup>21</sup>

The matrix (fiber cement without additive) was developed first by varying only the reinforcing fiber (NBSK) content (2–32 wt%). We postulated that to develop fiber cement high biomaterial content, the first step is to establish the baseline with a wide range of fiber content (Table 1). In such a way, we can optimize the formulation recipe with biobased binders, which is not limited to micro-cellulosic additives. However, high aspect ratio NBSK fibers in a cement matrix is challenging to disperse if superplasticizers are not used. Therefore, the upper limit was experimentally set at 32 wt% by testing different wood-based pulp fibers. Based on the exploratory work, we observed that the content of bleached and unbleached fibers (high aspect ratio) is possible to extend up to 32 wt%,<sup>29</sup> exhibiting comparable mechanical properties, *e.g.*, flexural strength. We want to note that such a range might vary for natural fibers with different (*i.e.*, low) aspect ratios.

Likewise, the high content of additives in a cement matrix also has detrimental effects, *i.e.*, cracking (Fig. S2†). Thus, the maximum allowable content for MCC (additive 2) was 10 wt%. In contrast, AC did not render cracking of the fiber cement (within the composition range). Thus, owing to these

**Table 1** List of specimens and the corresponding composition. The sample nomenclature and composition of all the fiber cement slurry and cured samples were prepared for this study

Sample ID	Cellulosic (NBSK) fibers (wt% of cement)	w/c ratio	Additive (wt% of cement)	
			AC	MCC
<b>Without additive</b>				
NBSK_2%	2 (8.4 g)	0.5	—	—
NBSK_4%	4 (16.8 g)	0.5	—	—
NBSK_6%	6 (25.2 g)	0.5	—	—
NBSK_8%	8 (33.6 g)	0.5	—	—
NBSK_10%	10 (42 g)	0.5	—	—
NBSK_12% (control sample)	12 (50.4 g)	0.5	—	—
NBSK_16%	16 (67.2 g)	0.5	—	—
NBSK_24%	24 (100.8 g)	0.5	—	—
NBSK_32%	32 (134.4 g)	0.5	—	—
<b>Combination 1: AC and NBSK</b>				
AC_2%	10 (50.4 g)	0.5	2 (8.4 g)	—
AC_4%	8 (33.6 g)	0.5	4 (16.8 g)	—
AC_6%	6 (25.2 g)	0.5	6 (25.2 g)	—
AC_8%	4 (16.8 g)	0.5	8 (33.6 g)	—
AC_10%	2 (8.4 g)	0.5	10 (42 g)	—
<b>Combination 2: MCC and NBSK</b>				
MCC_2%	10 (50.4 g)	0.5	—	2 (8.4 g)
MCC_4%	8 (33.6 g)	0.5	—	4 (16.8 g)
MCC_6%	6 (25.2 g)	0.5	—	6 (25.2 g)
MCC_8%	4 (16.8 g)	0.5	—	8 (33.6 g)



limitations, fiber cement with 12 wt% NBSK was chosen as the control, and the NBSK to additive (AC/MCC) weight was varied systematically so that the total biomaterial content remained at 12 wt%. For example, if NBSK is 6 wt% then additive is 6 wt%. Such variation afforded the physical effect of micro-cellulosic additives on the rheo-mechanical properties of the fiber cement to be observed. In terms terminology, combinations 1 and 2 corresponded to AC and MCC, respectively with NBSK fibers. Compositional details with sample nomenclature are illustrated in Table 1.

### 2.3 Physico-chemical characterization

**2.3.1 Attenuated total reflectance-Fourier transform infrared spectroscopy (ATR-FTIR).** The ATR-FTIR spectra of AC/MCC additives were obtained using a Bruker HCT Inventio ATR-FTIR spectrometer. The additives (used as received) were spread onto the ATR internal reflection element (diamond crystal). The recorded spectral range was from 600 to 4000  $\text{cm}^{-1}$  (4  $\text{cm}^{-1}$  resolution), with an average of 32 scans per sample. For brevity, only the mid IR range (600–2000  $\text{cm}^{-1}$ ) was shown to highlight the functional groups present in the micro-cellulosic additives (AC and MCC).

**2.3.2 Raman spectroscopy.** The Raman spectra of the micro-cellulosic additives (AC and MCC) were recorded using a dispersive Raman spectrometer from Wasatch Photonics, USA (model: WP 785). The specimen was loaded on a hollow stainless-steel holder and the surface was flattened with a spatula prior to the data acquisition. The recorded spectral range was from 250 to 2000  $\text{cm}^{-1}$  (8  $\text{cm}^{-1}$  resolution).

The solid particle/fiber was illuminated with a 785 nm laser since the cellulosic material can exhibit autofluorescence under 532 nm excitation. Now, as the Raman scattering intensity will be reduced under higher laser excitation, high (100%) laser power was chosen to achieve the best S/N ratio. To reduce the any-laser induced degradation, a spectrum was collected at 0.5 ms exposure time. An adaptive iterative penalty least squares method (air-PLS) as a background method was applied on the collected Raman spectra of the micro-cellulosic additives (AC and MCC).

### 2.4 Microstructural characterization

Microstructural characterization was performed using a Scanning Electron Microscope (SEM), from Hitachi, Japan (model: SU3500).

Cellulosic (micro and nano) materials are intrinsically non-conductive. As such, they were coated with a thin layer of iridium (Ir) nanoparticles (*ca.* 12 nm) using a sputter coater<sup>33</sup> from Leica Microsystems, Germany (model: EM MED020 coating system). The conductive coating suppresses the charging effect as well as beam-induced degradation, which is detrimental to the fragile fibers and soft micro-particles.

### 2.5 Particle/fiber size and shape characterization

Size and shape characterization of anisotropic particles and high aspect ratio fibers is inherently challenging using the traditional dynamic light scattering (DLS) technique. Though a static light

scattering (SLS) would be more suitable, considering the application prospects of the employed micro-cellulosic additives, a laser-diffraction based particle (and/or fiber) analyzer technique (solid-state) was adopted in this research.

The average particle diameter of the micro-cellulosic materials (AC/MCC) was measured using a dynamic image analyzer (DIA) from Sympatec GMBH, Germany (model: RODOS). Approximately 1 g of specimen was fed into a vibrating sample dispenser, which feeds the samples into the DIA for imaging and size analysis. One of the key advantages of using DIA is it accounts for the variation in the shape of the fiber and particle and is free of solvent-induced effects.

During the experiment, the sample feed rate was kept constant at 20% (with a gap width of 2 mm) and the particles were dispersed using 1 bar pressure and a vacuum pressure of 14 mbar. A system configuration of 175 Hz and trigger conditions were maintained at an optical concentration range of  $C_{\text{opt,start}} \geq 0.02\%$  to  $C_{\text{opt,end}} \leq 0.02\%$ . The accelerated individual particles (open jet aerosol) then pass through an image analyzer, and are then measured for their properties. The volume mean diameter (VMD) was computed by the software using the equal area projection method (EQPC).<sup>34,35</sup>

The shape descriptor of irregularly shaped particles was computed by calculating its fractal dimensions (Feret) and has a scale from (0–1). Note that '1' means the geometry resembles closely a fixed shape descriptor (*e.g.*, circle, sphere, and line) while closer to "0" indicates an increase in the complexity of the particle/fiber geometry. By default, the software in RODOS computes the fractal dimensions and provides a (0–1) comparison, indicating how complex a geometry the measured particle/fiber possesses. For instance, the aspect ratio\* is calculated by computing the maximum and minimum Feret dimensions and dividing them.

### 2.6 Rheological characterization

Rheological characterization was performed using a rotational rheometer from Netzsch, Germany (model: Malvern Kinexus ultra plus) with a vane-in-cup geometry (4 blades, 25 mm diameter, depicted in Fig. 2(a)). The rheological test plan was designed to understand the flow properties, *e.g.*, shear thinning and workability (estimation of the yield stress) of the fiber cement slurry. The tests were performed at room temperature ( $25 \pm 1^\circ\text{C}$ ) and the results were repeatable within  $\pm 5\%$ .

Note that all the fiber cement slurries (with and without additive) were assessed to evaluate the specimen at its dormant period, at an early age of  $10 \pm 1$  minute to ensure consistencies in data collection. This is a crucial factor since the cement hydration reaction proceeds at the dormant period, and cement starts to set (will harden eventually). Also, this would allow the normal force to reach zero under a stress-free resting period.<sup>36</sup>

The rheological experiments were performed under both oscillatory and rotational tests (see Fig. 2(b and c)). The amplitude sweep experiments were conducted at a constant frequency of 1 Hz, within the shear strain range of 0.01% to 1000% while steady-state viscometry was performed within the shear rates of 0.01–1000  $\text{S}^{-1}$ .



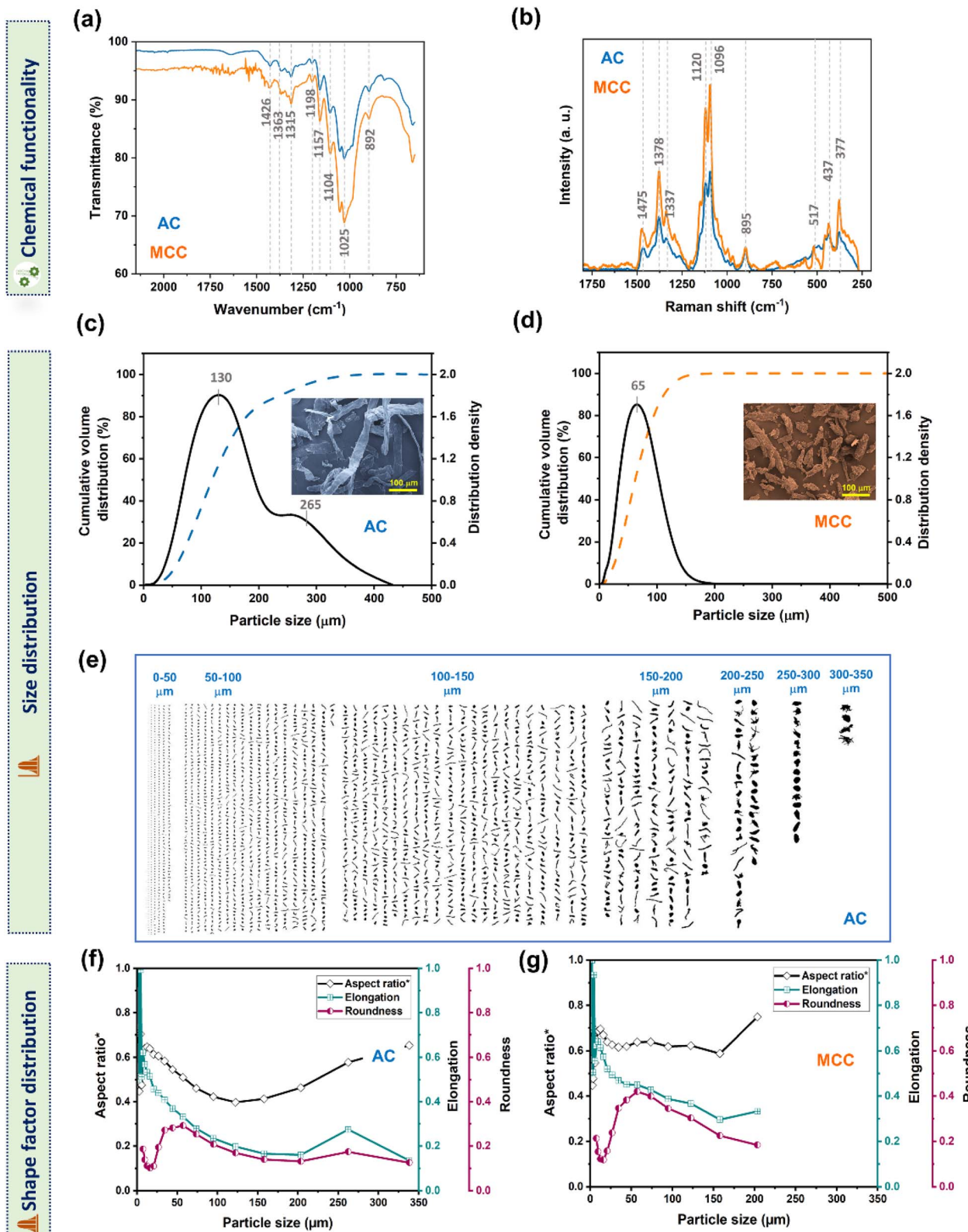


**Fig. 1** Solid-state physico-chemical characterization of micro-cellulosic additives (AC and MCC) using vibrational spectroscopy and laser-diffraction based particle/fiber shape analysis. (a) ATR-FTIR spectra. (b) Raman spectra highlighting the major vibrational bands. Particle/fiber size distribution (LEFI) curves. (c) AC and (d) MCC with inserted SEM micrographs (color coded to match the color of the distribution profiles). (e) Illustration of the DIA-enabled size distribution curve of AC with an individual particle/fiber captured during the measurement. Variation of shape descriptors (aspect ratio\*, elongation, roundness) with particle size of (f) AC and (g) MCC. Note that the mentioned VMD corresponds to the volume mean diameter, LEFI stands for length of fiber, and elongation is the ratio of DIFI (diameter of the fiber) to LEFI. See the experimental section for details on the aspect ratio\* (range: 0–1) calculation method.

## 2.7 Mechanical characterization

Mechanical characterization was performed using a Universal Testing Machine (UTM) from Instron, USA (model: 5969 dual column table frames; 50 kN capacity). Since fiber cement is utilized as a non-structural building material, it is more prone to bending failure. Low thickness (*i.e.*, 8 mm) and high span length induce bending moments more than compression, which is mostly associated with load-bearing applications. The flexural strength of the air-cured fiber cement composites was calculated based on the 3-point bending test. Note that the testing parameters were chosen based on the ASTM C1185 method. Thus, flexural property-related metrics, like the modulus of rupture (MOR), is considered for cost to performance evaluation (detailed in the Results and discussion section).

In all cases (unless stated otherwise), the fabricated composite (with and without additive) was removed from the mold after 28 days of curing, and then cut into rectangular blocks of size  $19.5 \times 4.5 \times 0.8 \text{ cm}^3$  before being fed into the UTM to obtain load *vs.* deflection curves and to calculate MOR.<sup>37</sup>

## 3 Results and discussion

### 3.1 Physico-chemical characterization

The chemical functionality of the cellulosic additives employed for this research was probed using complementary vibrational spectroscopic techniques, like ATR-FTIR and Raman. Fig. 1(a and b) illustrate the chemical “fingerprint” of AC and MCC, which are identical. It was not surprising as they bear similar functional groups, like hydroxy and glycosidic ether bonds (C–O–C). The IR spectra confirmed the presence of characteristic cellulosic bands, observed at 1025 and  $1155 \text{ cm}^{-1}$  corresponding to the C–C breathing mode and C–O–C, respectively. In Raman spectra, the symmetric and asymmetric stretching bands of C–O–C were observed at 1096 and  $1120 \text{ cm}^{-1}$ , respectively. Furthermore, the Raman spectrum shed more light on the crystalline structure (and orientation) of the polymorphic cellulose, which could be ascribed to cellulose I for both AC and MCC, based on the stretching frequencies at 377, 1096, 1378, and  $1475 \text{ cm}^{-1}$ , which was also observed previously for Avicel I.<sup>38</sup> Thus, based on the chemical analysis using surface-sensitive techniques, AC and MCC exhibit comparable features.

Physical properties, *e.g.* morphology, which is a crucial aspect for a composite's mechanical performance, could vary for cellulosic materials. Fig. 1(c and d) display the variability in morphology of the micro-cellulosic additives employed in this study. Structurally, both AC and MCC were fluffy fibrous-like, but the former was longer in length as compared to the latter. To further investigate their size disparity, solid-state particle/fiber size and shape analysis was performed as shown in Fig. 1(c and d). Notably, AC displayed a volume mean diameter (VMD) of 134  $\mu\text{m}$  with a bimodal distribution curve whereas for MCC, VMD was 64  $\mu\text{m}$  and size distribution was monomodal.

In terms of additive shape characteristics, Fig. 1(f and g) indicate the variation in shape descriptors (such as aspect

ratio\*, roundness, and elongation) with particle size. Key observations from Fig. 1(f and g) were that MCC is more spherical and less elongated in shape as compared to AC (less spherical and more elongated). Additionally, MCC exhibited uniformity (less variability in shape) whereas the AC shape descriptors, *e.g.* aspect ratio, vary drastically with particle size.

In-depth size and shape factor analysis is particularly critical when we analyse the flow behaviour (rheology) and mechanical characterization of cement composites containing AC and MCC as additives. Recent studies employed fractal dimensions to compute various shape descriptors of MCC samples to understand their flowability – with particle circularity or roundness contributing to the maximum effect.<sup>39</sup>

Therefore, these results suggest to us that the shape and size characteristics of AC and MCC could play a crucial role in imparting specific properties<sup>40</sup> to the fiber cement, discussed in the coming sections. Additionally, the variation of particle shape with respect to particle size can provide valuable insights on the strengthening mechanism of biobased additives in the cementitious composite.

### 3.2 Rheological characterization

Understanding the rheology of fiber cement suspension is important to its manufacturing process, as the transportation, handling, and storage of the slurry in a facile manner could aid in reducing its processing costs. Among the different rheological features of cement pastes, the shear-thinning properties and yield stress are of great importance not only for transportation purposes but also for formulation and processing.<sup>41</sup> The former quantitatively explains the decrease in viscosity of the slurry upon agitation and the latter elucidates the integrity of the slurry at rest.

During the fiber cement manufacturing (*i.e.*, Hatschek process),<sup>2</sup> after mixing, the fiber-cement slurry is transported to the processing line where it will undergo various steps. Yield stress (stress that must be applied before the material starts to flow) is particularly important when it comes to processing flexibility such as the workability of the cement/fiber-cement slurry – optimum yield stress ensures workability,<sup>42</sup> segregation resistance (a non-homogeneous mix affecting the mechanical strength), bleeding resistance<sup>43</sup> (free water that comes out from the slurry during consolidation), setting time<sup>41</sup> and consolidation (formwork stability) of the cement pastes.<sup>44</sup>

Fig. 2 illustrates the evolution of yield stress as a function of the content of the micro-cellulosic additive (AC and MCC). There exists a wide range of methods for calculating yield stress in the literature such as creep, cross-over of amplitude sweep, stress ramp, and frequency sweep.<sup>45</sup> Here, we calculated the “yield point” *via* two different methodologies (*vide infra*) known as cross-over of amplitude sweep moduli<sup>46</sup> and curve-fitting on the steady-state viscometry results.<sup>47</sup> As presented in Fig. 2(b), using amplitude sweep results, the transition point from a viscoelastic solid ( $G' > G''$ ) to a liquid-like state ( $G'' > G'$ ) may be used as a direct method to measure the “yield point”. On the other hand, by fitting the Herschel–Bulkley model on the steady viscometry results, one may indirectly estimate the yield point



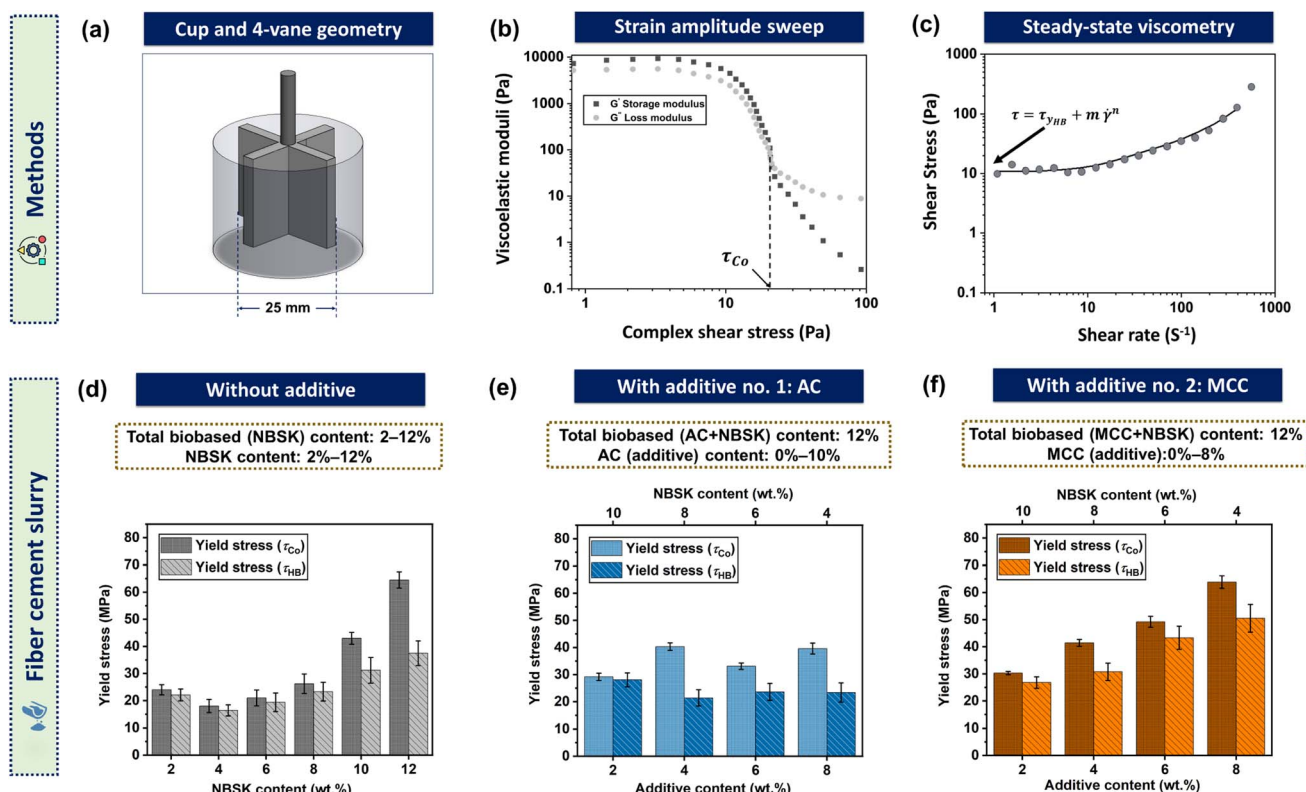


Fig. 2 Rheological characterization of the fiber cement slurry. (a) The cup and 4 vane rheometer geometry. Methods of computing yield stress using (b) the direct method—strain amplitude sweep, and (c) indirect method—steady state viscometry (Herschel–Buckley model). Reinforcing (NBSK) fiber/additive content dependent yield stress of the fiber cement slurry without additive, (d) NBSK; with micro-cellulosic additive, (e) AC (combination 1: AC and NBSK), and (f) MCC (combination 2: MCC and NBSK).

as shown in Fig. 2(c). This rheological model can be described as follows:

$$\tau = \tau_{yHB} + m\dot{\gamma}^n \quad (1)$$

where  $\tau$  is the shear stress,  $\tau_{yHB}$  is yield stress,  $m$  is the consistency coefficient,  $\dot{\gamma}$  is the shear rate and  $n$  represents the flow index.<sup>48</sup>

As observed in Fig. 2(d–f), irrespective of the methods, the “yield point” follows the same trend as a function of the content of the cellulose-based additives (AC and MCC). Note that the yield stress measured by the cross-over method is higher than the one measured by curve-fitting. The difference between the two yield points has been previously reported in the case of other slurries and suspensions. For some fluids, the cross-over of the amplitude sweep is beyond the true “yield point” of the system, introducing a larger magnitude of yield stress.<sup>46</sup> On the other hand, there exist some discrepancies in measuring the “yield point” using curve-fitting—its magnitude is highly dependent on the range of data points and the quality of data acquisition under low shear rates.<sup>49</sup>

Fig. 2(d) represents the yield stress trend of cement paste (without additive) containing varying amounts of NBSK. Notably, with increment of the NBSK content, yield stress exhibited increasing trend, and was maintained up to 8 wt% after which yield stress increases drastically—it reached

a maximum of 65 Pa at 12 wt% NBSK. Such observations are common in the rheology of pulp fiber suspensions. Note that the high aspect ratio pulp fibers tend to undergo bridging and interlocking effects and have high van der Waals' forces of attraction between fibers.<sup>50</sup> Thus, it creates resistance to the flow of any suspension including cement paste, and thereby increase the yield stress.<sup>51</sup> Also, long fibers increase the fiber cohesion,<sup>50</sup> which can be a contributing factor to the aggregated state of the cement particles—yield stress increases.<sup>51–53</sup> Moreover, high content of pulp fibers will inadvertently result in less spacing between the fibers within the cement matrix, thereby resulting in a possible hinging/bending effect between fibers—yield stress increases.<sup>52–54</sup> To summarize, yield stress strongly depends on the content of the reinforcing (NBSK in this case) fibers, and since no conventional superplasticizer was employed, to understand the effect of micro-cellulosic additives, the maximum NBSK content was set at 12 wt% for the rheological (also for mechanical, explained in the respective section) characterization. Also, it is reasonable to benchmark the performance metrics of the fiber cement with nano-cellulosic additives.<sup>21</sup>

Fig. 2(e) illustrates the trends in yield stress variation of the fiber cement slurry as a function of AC content (2–10 wt%) while keeping the total biomaterial content fixed at 12 wt%. From an absolute point of view, yield stress was low for all the



combinations of AC and NBSK (binary materials) as compared to NBSK (unary biomaterial). But it is interesting to note that it was varied within a narrow range (30–45 Pa) with a maximum of 45 Pa at 6 wt% AC content. Such a trend could be attributed to the stabilizing agent role of AC, which can improve dispersion, resulting in a uniform mix of the components in the fiber cement slurry. Also, due to the lower crystallinity than MCC (see Fig. S4†), AC affords better water retention. Note that AC is typically used as a stabilizing agent in pharmaceutical applications wherein it facilitates controlled release of water/moisture with time.<sup>55</sup> This could perhaps mean that the increase in yield stress due to the presence of pulp fibers can be negated by the controlled addition of AC into the mixture, thereby keeping the yield stress values at usable regimes preventing a rapid increase of yield stress and viscosity. Also as observed from Fig. 1(c–f), AC consists of a short fiber-like morphology (elongated and less spherical in shape) and so the fiber cohesion between them tends to be minimal compared with macro pulp fibers (high van der Waals' attraction). As a result, the mix consisting of fibers and AC is less prone to getting entangled, resulting in an improved dispersion, and contributing to the reduction in yield stress.

Finally, as displayed in Fig. 2(f), yield stress was steadily increased for the fiber cement slurry with MCC (content: 2–10 wt%), and the maximum yield stress of 64 Pa was observed at 8 wt% MCC. These results were consistent with the results obtained from the studies conducted by Cao *et al.*, wherein they found that for a fixed water–cement (w/c) ratio of 0.35, the incorporation of CNC in cement paste increased the yield stress from 15 Pa (at 0.04 vol%) to 600 Pa at 0.15 vol% CNC concentration.<sup>20</sup> They have hypothesized this was due to the agglomeration effect of CNC in fresh cement paste pore solution.<sup>20</sup> We believe that such a mechanism may play a pivotal role in increasing the yield stress in the case of MCC (combination 2 in this study) despite not being nanoscale cellulosic materials. However, MCC has similar physico-chemical properties, like hydrophilicity, crystallinity and narrow particle size distribution as compared to AC.

Overall, it can be inferred from the rheological studies that AC and NBSK (combination 1) are more effective than MCC and NBSK (combination 2) in reducing the yield stress (improving the workability) of the fiber cement slurry as compared to MCC.

### 3.3 Mechanical characterization

The strength of a fiber cement composite is crucial as it dictates the feasibility in terms of design, performance, durability, and quality for a particular building material application, *i.e.*, external cladding/façade materials. As such, they are more prone to bending (flexural) failure as compared to compression failure (associated with load-bearing components). Factors such as wind loadings, thermal expansion (freeze–thaw), and moisture absorption (wet/dry cycles), to name a few, significantly contribute to flexural loadings when fiber cement is draped around a building structure.<sup>56</sup> Hence, cement, which is inherently brittle, is reinforced *via* high-aspect ratio fibers to improve its ductile by promoting strain hardening.<sup>29</sup> The incorporation of

micro-cellulosic biomaterials (as additives) can further alter this behavior depending upon their type, nature, and concentration.

From Fig. 3(a), as the reinforcement content increases (8–32%), a decrease in peak strength with an increase in strain hardening behaviour was observed. Pulp fibers enhance the strain-hardening and load transfer ability of cement composites by forming networks that bridge the crack during deformation/failure. However, exceeding a feasible limit can cause weak points within the composite itself, resulting in agglomeration (dispersion challenges) and eventually leading to the failure of the composite. Therefore, based on this observation and being cognizant about the processing challenges without the conventional superplasticizer, the upper limit of the NBSK was 32 wt%. However, to be consistent with the rheological characterization, we chose 12 wt% as the limit for total biomaterial (binary components) content for mechanical tests (*vide infra*).

Fig. 3(b and c) depict the flexural stress–strain behavior of fiber cement with micro-cellulosic additives, which are AC (combination 1) and MCC (combination 2), respectively. Interestingly, the strain-hardening region and ductility is indeed highest for the control fiber cement (without additive), which is not surprising as it has the maximum reinforcement. This could be primarily due to the different reinforcing mechanism in the presence of additives (AC/MCC), which will be discussed in the following section. In Fig. 3(b), with the addition of AC (2–4 wt%), the ductility and strain hardening region reduced although the peak strength was improved. At low content, AC functioned as an inert filler (see Fig. 1(d) and S3†), which densifies the composite, while it reduces strain-hardening but improves the peak strength. On the other hand, at higher AC content (*i.e.*, 6–8 wt%), an improvement was observed with both peak strengths as well as the strain-hardening behavior. This could be due to the fibrous nature and larger size of AC (see Fig. 1(e) and S3†), which in combination with NBSK fibers can form network structures (this could be a fiber–matrix interlocking network (mechanical interlock) or microfibrillar networks formed between cellulose fibers (chemical interlock), thereby improving the reinforcing ability (by bridging cracks and resisting deformation under load) which makes the composite more ductile). Note that a maximum MOR of 7.9 MPa is observed at 6 wt% AC in high-density fiber cement. This originates from the combination of macro–micro reinforcement (combination 1: AC and NBSK) mechanism as evidenced previously for the CNC and NBSK combination.<sup>21</sup>

Based on the MOR data (Fig. 3(d–f)), it is our speculation that the presence of a sufficient amount of cellulosic additive (*i.e.*, >4 wt% for AC) has an important role to play in maximizing the flexural strength, which would be governed by its morphology and size. In particularly for fiber cement with AC, potential longer cracks are mitigated by the bridging effect of the high aspect-ratio NBSK fibers. Besides, AC can suppress the micro-scale cracks by bridging the micro-cracks. However, upon exceeding the limit, which is 10 wt% in this case, MOR was decreased due to stress concentration within the span of the composite, compromising its flexibility.<sup>20</sup> However, we note that the sufficient content of a particular additive will vary if any of the parameters in the formulation changes, hence, at this



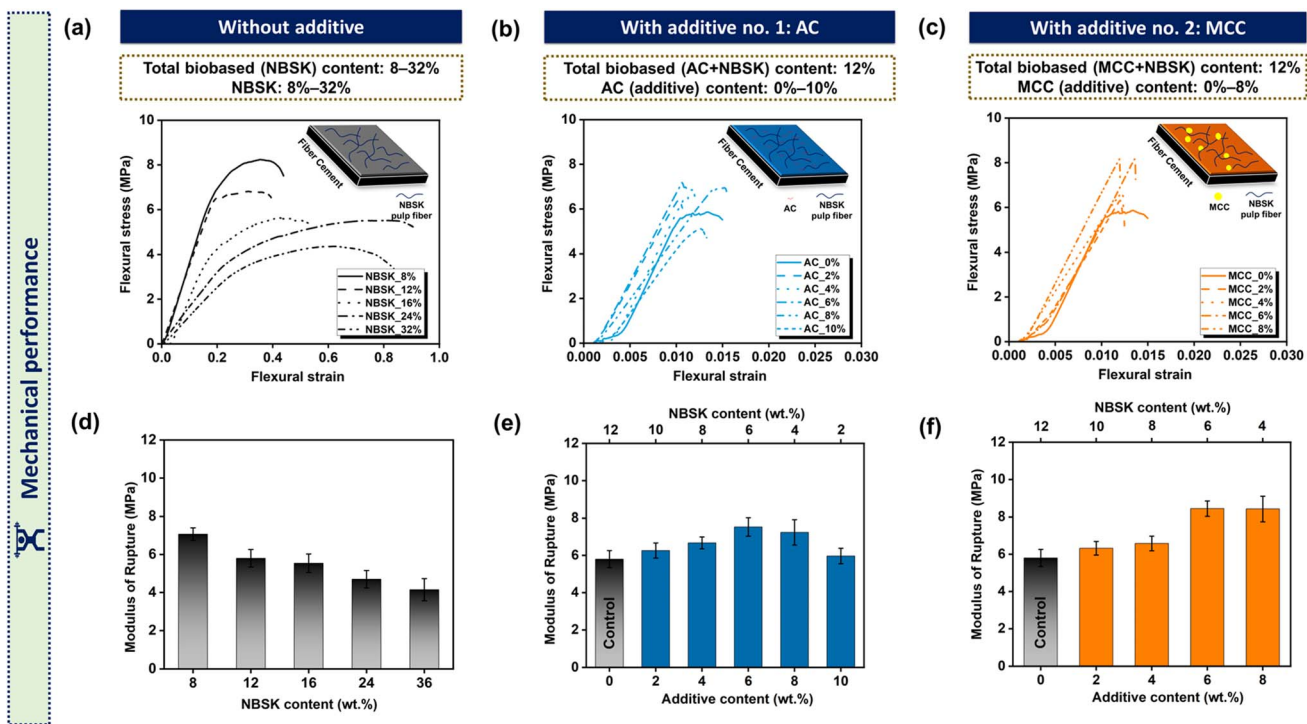


**Fig. 3** Mechanical characterization of the fiber cement. Representative flexural stress–strain curves (a–c) and modulus of rupture (MOR) bar charts (d–f) of cured (28 days) composites. Reinforcing (NBSK) fiber/additive content dependent stress–strain curves and modulus of rupture (MOR) charts of the fiber cement slurry without additive: (a and d) NBSK; with micro-cellulosic additive, (b and e) AC (combination 1: AC and NBSK), and (c and f) MCC (combination 2: MCC and NBSK). The “control sample” refers to a fiber cement specimen without any additive, ca. 12 wt% NBSK fibers. Fiber cement with micro-cellulosic additives (AC and MCC), the fiber-to-additive content is varied in such a way that the total biobased content remains at 12 wt%. There is one data point missing in (c)–(f) for MCC owing to the failed curing of the composite (see Fig. S2† for visual confirmation).

juncture, we believe there is still scope for new ideas (and evidence) to further understand the failure mechanism of micro-cellulosic additives, which is beyond the scope of this study.

Fiber cement with MCC exhibited brittle fracture (irrespective of content) as compared to AC, with the increase in the peak strength and MOR. Smaller size and uniform shape characteristics of MCC (see Fig. 1(d and g) and S3†) densify the cement matrix by filling micro/nano scale voids present in the matrix. Hence, the composite becomes brittle. Fig. 3(f) also illustrates MCC content dependent variation in the MOR. At first, it increased from 6.3 MPa to 6.5 MPa (2–4 wt% MCC) while exhibiting a sudden increase from 6.5 MPa to 8.3 MPa, and then stabilized at 8.4 MPa (6–8 wt% MCC). These results were similar to the results observed in recent studies with the addition of MCC on the strength of the geopolymers-ordinary Portland cement system.<sup>32</sup> The study revealed that the addition of MCC improved the 7 day strength, after which it was dropped due to the chemical degradation of MCC.<sup>32</sup> Likewise, in a study conducted by Souza *et al.*, a combination of CNF (cellulose nanofibrils)/MCC resulted in increasing the MOR (70% increase at 0.075 wt%) of the composite.<sup>37</sup> The mechanism of strength development in MCC (hydrophilic) could also be due to improved hydration. Prior studies with CNC have shown such improvement in hydration, contributing to improved flexural

strength of cement composites.<sup>20,21</sup> Their affinity towards water enables them to channel water from hydrated (pore solution) to unhydrated regions during cement hydration.<sup>20,21</sup> As such, the mechanism was termed as short circuit diffusion (SCD).<sup>20</sup>

Moreover, the observed consolidation of MOR values at 6–8 wt% MCC content as shown in Fig. 3(f) is quite interesting. The reason could be that the effective MCC content that encounters cement particles, which modifies cement properties, may have saturated at 6 wt% MCC. Further addition of MCC to 8 wt% might just function as excess MCC in the cement matrix, which increases the yield stress as observed in Fig. 2(f) but with no further improvement in MOR. It is crucial to mention that upon increasing MCC content above 8 wt%, the sample cracked during curing, which could be due to the increased water demand, poor workability, and drying shrinkage effect, to name a few (see Fig. S2†). This tells us that we do not need to employ an exceedingly high content of MCC to facilitate the improved mechanical properties of fiber cement.

We also compared our current results with our past work,<sup>21</sup> wherein we benchmarked our results with fiber cement with CNC<sup>21</sup> and a commercially available polycarboxylate based (PCE) superplasticiser (see Fig. S5† for details).<sup>21</sup> Comparison of our current results with fiber cement with PCE illuminated the beneficial role of micro-cellulosic additives in the mechanical



performance (MOR) of fiber cement, thereby once again iterating the potential of these low-cost cellulose based additives in replacing conventionally employed petrochemical based additives in the cement/construction industry.

### 3.4 Strength to weight (S/W) analysis

In Fig. 4(a and b), the addition of both AC/MCC in varied proportions with NBSK improved the strength-to-weight ratio of the fiber cement. However, despite an increase in MOR observed with FC samples containing MCC (*versus* combination 2), the strength-to-weight ratio was within the same range (0.09–0.12) for FC samples containing both additives. This tells us that the addition of AC reduced the weight of the fiber cement composites whereas the weight of the composite increased with the addition of MCC. This can be attributed to the morphological difference between MCC and AC (Fig. 1(c–f) and S3†) resulting in high packing density.<sup>58</sup> These results are encouraging from an application standpoint, wherein the high strength-to-weight ratio plays a pivotal role in various industries, *e.g.*, construction<sup>59</sup> (promotes the ease of handling of high-rise buildings), aerospace/automobile<sup>60,61</sup> (increased payload capacity) and also in specialized applications in challenging environments like offshore marine/construction work, where buoyancy is an important factor.<sup>62</sup>

### 3.5 Cost to performance (C/P) analysis

Cost is one of the most important parameters that dictates the viability of commercialization at the industrial scale. Especially when it comes to the construction industry, the price of raw materials should be as low as possible, and scalability is a crucial aspect in the raw material production process. Considering these prospects, we leveraged the findings of this

study to conduct a simple cost/performance (C/P) analysis to deem which cellulose-based fiber/additive combination would be the most efficient, in terms of cost/performance (*vide infra*).

Note that the raw material cost (Table S12†) is adapted from previous in-depth techno-economic analysis conducted to ascertain their cost of production. To simplify the analysis, we have chosen samples from both combinations (1 and 2) that exhibited the best mechanical properties (Fig. 3(e) and (f)) and drawn a comparison with the control sample. To obtain a broader perspective, we considered the findings from our previous work on fiber cement with the combination of CNC and NBSK.<sup>21</sup> Now, to compare, we calculated the yield stress of the sample containing CNC based on the strain amplitude method mentioned in the experimental section as well (see Table S9†).

As shown in Fig. 5, by supplementing the NBSK fibers in proportions with other crystalline cellulose-based additives the total cost of the reinforcement/additive in the system can be reduced (40% cost reduction) with an increase in MOR by 34% when combination 1 is incorporated (*vs.* control sample). On the other hand, in the case of combination 2 (MCC and NBSK), both cost (20%) and MOR (45%) increase (*vs.* control). This means that the rise in the cost for adding MCC is possible to compensate by the improved mechanical performance in addition to its role in modifying the rheology of the fiber-cement slurry. The incorporation of both AC and MCC reduced the yield stress of the fiber-cement slurry (with a maximum reduction of 30% and 1.5%, respectively *vs.* control).

With regards to the CNC–NBSK combination, previous research<sup>21</sup> demonstrated a maximum increase in MOR by 46% (*vs.* control), whereas the yield stress increased by 17% (*vs.* control). However, the downside to CNC is its cost of

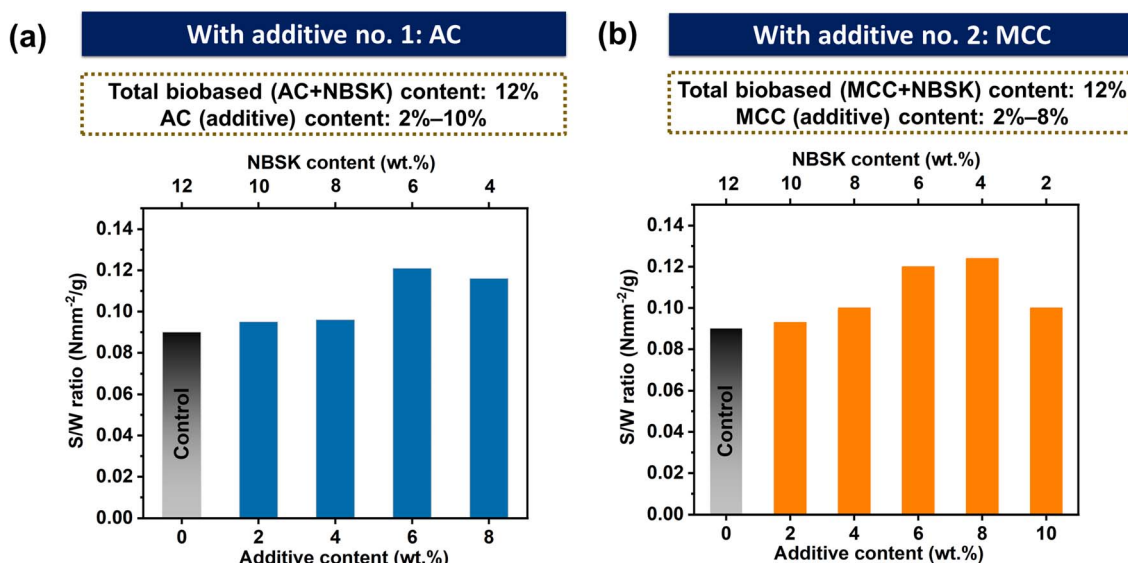


Fig. 4 Strength-to-weight (S/W) ratio analysis of fiber cement with micro-cellulosic additive (AC and MCC). (a) Combination 1 (AC and NBSK), (b) combination 2 (MCC and NBSK). Note that the ratio here refers to the mean modulus of rupture (MOR) values (in MPa) obtained from the three-point bending test (*vide supra*) to the weight (g) of the specimen used for the mechanical characterization (Fig. 3). At MCC content of 10 wt%, the specimen cracked before curing (see Fig. S2†).

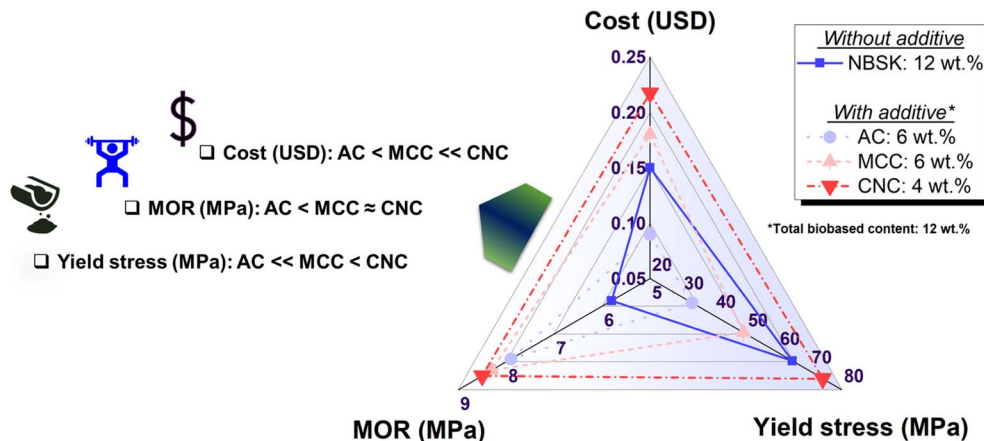


Fig. 5 Cost to performance (C/P) analysis of fiber cement with micro-cellulosic additives (AC and MCC). Spider chart depicting the C/P (performance corresponds to yield stress and MOR). Note that the cost here refers to the total reinforcement/additive cost—it does not include the cost of other raw materials and processing. In the ESI, Table S11† has the detailed background information.

production;<sup>22</sup> though AC is majorly found in wood pulp,<sup>63</sup> it can be extracted from inexpensive biomass sources, *e.g.* cotton,<sup>64</sup> improving its economic value proposition for mass production. Note that MCC could be derived from AC using mild acid hydrolysis<sup>65</sup> as mentioned in earlier sections. We also note that the maximum MOR values from Fig. 3(d–f) suggest that there isn't a significant difference between the flexural strength of the fiber cement when either CNC or micro-cellulosic biomaterials (AC/MCC) are employed, suggesting that, even by incorporating cost-efficient additives, desirable mechanical properties are possible to achieve.

Finally, Fig. 5 summarises the comparison of the C/P of FC samples (based on our current study) using a spider chart. Ideally, the best C/P samples would exhibit low cost and high strength with optimum yield stress. High yield stress would mean that more energy (which adds to the processing cost) would require the mixing/pumping of the fiber-cement slurry. Therefore, based on these considerations, we infer from Fig. 5 that, combination 1 (AC and NBSK) exhibited the best C/P proposition, followed by combination 2 (MCC and NBSK) and the CNC–NBSK combination. Thus, this analysis iterates the tremendous possibilities of employing additives from biomass sources (*i.e.*, polysaccharides-based) to develop cost-efficient, lightweight, and high-density fiber cement for a sustainable future.

## 4 Conclusion

Owing to the current environmental concerns, the exploration of renewable biomaterials for hard-to-abate cement-based building materials is warranted while offering reasonable cost-to-performance metrics. In this research, we have explored the paradigms of micro-cellulosic biomaterials as additives and their influence on the rheo-mechanical properties of fiber cement in which traditional materials of choice are either carbon-intensive or carcinogenic.

The key findings of this research are listed below:

(I) Rheological characterization revealed that incorporation of both combinations 1 and 2 resulted in a reduction in yield stress with combination 1 (NBSK and AC) indicating maximum reduction in yield stress (30%) of the fiber cement slurry (*vs.* control) and combination 2 resulting in a percentage reduction of 1.5%. The reasonably high crystallinity and morphological (shape and size) variety of cellulosic additives endow upon them the capability to impart distinctive rheological characteristics to the fiber cement slurry.

(II) Mechanical characterization revealed that incorporating AC/MCC in combination with NBSK fibers contributed to the improvement in the flexural strength: an increase of 34% for combination 1 (NBSK and AC) and 42% for combination 2 (NBSK and MCC). In addition to the strength improvement, addition of AC also improved the ductility of the fiber cement composite as compared to MCC addition, which made the composite more brittle. Herein, morphology played an important role and AC and MCC can induce different reinforcing effects on the fiber cement composite. Finally, we hypothesize that being more microfibrillar and larger compared to MCC, AC strengthens fiber cement differently in combination with NBSK as the reinforcing fiber. Also, results from strength-to-weight ratio analysis indicated that samples with AC can produce lightweight strength fiber cement composites (*vs.* samples containing MCC, CNC and control).

(III) There was a correlation between yield stress and modulus of rupture, which indicated that the yield stress and MOR were independent of AC content, whereas both increased with an increase in MCC content.

(IV) Cost-to-performance analysis revealed that a combination of additives (AC/MCC) with NBSK fibers can afford a high-density (total biomaterial content is >10 wt%) fiber cement with a 40% reduction in cost (combination 1: AC and NBSK) and 34% increase in MOR. Such an analysis alludes to the techno-economic benefit of micro-cellulosic additives, *i.e.*, AC.

Overall, the interesting findings of this research will accelerate our efforts in developing commercial-ready cement-based composite materials—lightweight yet strong; benign to the



environment yet functional—crucial to achieving SDGs for a healthier environment and ecosystem.

## Data availability

The data supporting this article have been included as part of the ESI† and in the main body of the manuscript.

## Author contributions

Conceptualization: S. R. and M. H., methodology: S. R., M. H., A. G. & B. Z., formal analysis: S. R., B. Z. & A. G., validation: S. R., M. H. & B. Z., visualization: S. R., writing – original draft: S. R., writing – editing: S. R. & M. H., funding acquisition and supervision: E. J. F. All authors read and approved the final manuscript.

## Conflicts of interest

There are no conflicts to declare.

## Acknowledgements

Authors gratefully acknowledge the financial support provided by the NSERC Canfor Industrial Research Chair in Advanced Bioproducts (#553449-19), the NSERC Discovery Grant (RGPIN-2021-03172), the Canada Foundation for Innovation (Project Number 022176), and Pacific Economic Development Canada (PaciFiCan). The authors also express their gratitude for the technical and instrumental assistance provided by Anita Lam of the XRD Laboratory, Department of Chemistry, University of British Columbia, Canada.

## References

- 1 Sustainable consumption and production, <https://www.un.org/sustainabledevelopment/sustainable-consumption-production/>, accessed 14 January 2024.
- 2 Z. Ranachowski, *The fabrication, testing and application of fibre cement boards*, 2018, vol. 125, ISBN:1-5275-0576-6.
- 3 D. D. L. Chung, *Carbon Compos.*, 2017, 333–386.
- 4 R. El-Sheikhy, *Sci. Rep.*, 2023, 13(1), 1–27.
- 5 R. Bouras, A. Kaci and M. Chaouche, *Korea Aust. Rheol. J.*, 2012, 24, 35–44.
- 6 M. Palacios and R. J. Flatt, *Science and Technology of Concrete Admixtures*, 2016, pp. 415–432.
- 7 M. G. Altun, S. Özen and A. Mardani-Aghabaglou, *Constr. Build. Mater.*, 2020, 246, 118427.
- 8 J. G. H. Antoni, O. C. Kusuma and D. Hardjito, *Procedia Eng.*, 2017, 171, 752–759.
- 9 J. Y. Shin, J. S. Hong, J. K. Suh and Y. S. Lee, *Korean J. Chem. Eng.*, 2008, 25(6), 1553–1561.
- 10 S. Ng and H. Justnes, *J. Sustainable Cem.-Based Mater.*, 2015, 4, 15–24.
- 11 D. F. Zhang, B. Z. Ju, S. F. Zhang, L. He and J. Z. Yang, *Carbohydr. Polym.*, 2007, 70, 363–368.
- 12 J. G. Vieira, G. d. C. Oliveira, G. R. Filho, R. M. N. de Assunção, C. da S. Meireles, D. A. Cerqueira, W. G. Silva and L. A. d. C. Motta, *Carbohydr. Polym.*, 2009, 78, 779–783.
- 13 A. Engbert, S. Gruber and J. Plank, *Carbohydr. Polym.*, 2020, 236, 116038.
- 14 X. Chen, M. G. Matar, D. N. Beatty and W. V. Srubar, *ACS Sustain. Chem. Eng.*, 2021, 9, 13726–13734.
- 15 A. Peschard, A. Govin, J. Pourchez, E. Fredon, L. Bertrand, S. Maximilien and B. Guilhot, *J. Eur. Ceram. Soc.*, 2006, 26, 1439–1445.
- 16 M. Penkała, P. Ogorodnik and W. Rogula-Kozłowska, *Pol. J. Environ. Stud.*, 2019, 28, 4057–4071.
- 17 S. Bourbia, H. Kazeoui and R. Belarbi, *Mater. Renew. Sustain. Energy*, 2023, 12(2), 117–139.
- 18 M. Smirnova, C. Nething, A. Stolz, J. A. D. Gröning, D. P. Funaro, E. Eppinger, M. Reichert, J. Frick and L. Blandini, *npj Mater. Sustain.*, 2023, 1(1), 1–15.
- 19 M. Smirnova, C. Nething, A. Stolz, J. A. D. Gröning, D. P. Funaro, E. Eppinger, M. Reichert, J. Frick and L. Blandini, *npj Mater. Sustain.*, 2023, 1(1), 1–15.
- 20 Y. Cao, P. Zavaterri, J. Youngblood, R. Moon and J. Weiss, *Cem. Concr. Compos.*, 2015, 56, 73–83.
- 21 S. Raghunath, M. Hoque and E. J. Foster, *ACS Sustain. Chem. Eng.*, 2023, 11(29), 10727–10736.
- 22 C. Abbati De Assis, C. Houtman, R. Phillips, T. Bilek, O. J. Rojas, M. S. Peresin, H. Jameel and R. Gonzalez, *Biofuels, Bioprod. Bioref.*, 2017, 11(4), 682–700.
- 23 H. Shaghaleh, X. Xu and S. Wang, *RSC Adv.*, 2018, 8, 825–842.
- 24 L. Lei, T. Hirata and J. Plank, *Cem. Concr. Res.*, 2022, 157, 106826.
- 25 H. Rivai, A. S. Hamdani, R. Ramdani, R. S. Lalfari, R. Andayani, F. Armin and A. Djamaan, *Technological Innovation in Pharmaceutical Research*, 2021, vol. 3, pp. 68–75.
- 26 O. A. Adeleye, O. A. Bamiro, D. A. Albalawi, A. S. Alotaibi, H. Iqbal, S. Sanyaolu, M. N. Femi-Oyewo, K. O. Sodeinde, Z. S. Yahaya, G. Thiripuranathar and F. Menaa, *Materials*, 2022, 15, 5992.
- 27 X. Truong Nguyen, US7005514B2 – Process for preparing microcrystalline cellulose – Google Patents, <https://patents.google.com/patent/US7005514B2/en>, accessed 3 December 2023.
- 28 Y. Sumra, S. Payam and I. Zainah, *J. Wuhan Univ. Technol., Mater. Sci. Ed.*, 2020, 35(5), 908–924.
- 29 M. Hoque, S. Kamal, S. Raghunath and E. J. Foster, *Sci. Rep.*, 2023, 13(1), 1–13.
- 30 L. R. Van Loon, M. A. Glaus, A. Laube and S. Stallone, *J. Environ. Polym. Degrada.*, 1999, 7, 41–51.
- 31 C. Gómez Hoyos, E. Cristia and A. Vázquez, *Mater. Des.*, 2013, 51, 810–818.
- 32 S. Rocha Ferreira, N. Ukrainczyk, K. Défáveri do Carmo e Silva, L. Eduardo Silva and E. Koenders, *Constr. Build. Mater.*, 2021, 288, 123053.
- 33 R. Heu, S. Shahbazmohamadi, J. Yorston and P. Capeder, *Microsc. Today*, 2019, 27, 32–36.
- 34 R. Xu and O. A. Di Guida, *Powder Technol.*, 2003, 132, 145–153.



35 RODOS, <https://www.sympatec.com/en/particle-measurement-dispersing-units/rodos>, accessed 27 August 2024.

36 D. Han and R. D. Ferron, *Constr. Build. Mater.*, 2015, **93**, 278–288.

37 ASTM International, *ASTM C1185 Standard Test Methods for Sampling and Testing Non-Asbestos Fiber-Cement Flat Sheet, Roofing and Siding Shingles and Clapboards*, 2016.

38 J. H. Wiley and R. H. Atalla, *Carbohydr. Res.*, 1987, **160**, 113–129.

39 H. Xiu, F. Ma, J. Li, X. Zhao, L. Liu, P. Feng, X. Yang, X. Zhang, E. Kozliak and Y. Ji, *Powder Technol.*, 2020, **364**, 241–250.

40 M. Kurpińska, M. Pawelska-Mazur, Y. Gu and F. Kurpiński, *Sci. Rep.*, 2022, **12**(1), 1–14.

41 W. Mbasha, I. Masalova, R. Haldenwang and A. Malkin, *Appl. Rheol.*, 2015, **25**, 9–19.

42 B. Feneuil, N. Roussel and O. Pitois, *Cem. Concr. Res.*, 2019, **120**, 142–151.

43 A. Perrot, T. Lecompte, H. Khelifi, C. Brumaud, J. Hot and N. Roussel, *Cem. Concr. Res.*, 2012, **42**, 937–944.

44 J. Mzwandile, M. Willy and H. Rainer, *Constr. Build. Mater.*, 2023, **393**, 131917.

45 B. Zakani and D. Grecov, *Cellulose*, 2020, **27**, 9337–9353.

46 M. Dinkgreve, J. Paredes, M. M. Denn and D. Bonn, *J. Non-Newton. Fluid Mech.*, 2016, **238**, 233–241.

47 P. Moller, A. Fall, V. Chikkadi, D. Derkx and D. Bonn, *Philos. Trans. R. Soc., A*, 2009, **367**, 5139–5155.

48 F. De Larrard, C. F. Ferraris and T. Sedran, *Mater. Constr.*, 1996, **31**, 494–498.

49 D. De Kee, Yield stress measurement techniques: A review, *Phys. Fluids*, 2021, **33**(11), 111301.

50 U. Hirn and R. Schennach, *Sci. Rep.*, 2015, **5**(1), 1–9.

51 T. Wikström and A. Rasmussen, *Nord. Pulp Pap. Res. J.*, 1998, **13**, 243–250.

52 C. P. J. Bennington, R. J. Kerekes and J. R. Grace, *Can. J. Chem. Eng.*, 1990, **68**, 748–757.

53 B. Derakhshandeh, S. G. Hatzikiriakos and C. P. J. Bennington, *J. Rheol.*, 2010, **54**, 1137–1154.

54 B. Derakhshandeh, R. J. Kerekes, S. G. Hatzikiriakos and C. P. J. Bennington, *Chem. Eng. Sci.*, 2011, **66**, 3460–3470.

55 J. Shokri, K. Adibkia, J. Shokri and K. Adibkia, *Medical Cellulose, Pharmaceutical and Electronic Applications*, 2013, DOI: [10.5772/55178](https://doi.org/10.5772/55178).

56 A. Adamczak-Bugno, G. Świt, A. Krampikowska and E. Proverbio, *Materials*, 2022, **15**, 5757.

57 L. O. de Souza, M. Liebscher, L. M. S. de Souza, F. de Andrade Silva and V. Mechtcherine, *Constr. Build. Mater.*, 2023, **408**, 133812.

58 L. Silva, S. Parveen, A. Filho, A. Zottis, S. Rana, R. Vanderlei and R. Fangueiro, *Powder Technol.*, 2018, **338**, 654–663.

59 M. Sifan, B. Nagaratnam, J. Thamboo, K. Poologanathan and M. Corradi, *Constr. Build. Mater.*, 2023, **362**, 129628.

60 J. Adel, K. Trottman, V. French, S. Raghunath, F. Brito dos Santos and E. Johan, *Polym. Compos.*, 2024, 1–14.

61 W. Zhang and J. Xu, *Mater. Des.*, 2022, **221**, 110994.

62 J. B. Yan, J. Y. Wang, J. Y. R. Liew and X. Qian, *Constr. Build. Mater.*, 2016, **111**, 774–793.

63 WIPO|PCT, WO2012/070072A2, 2011.

64 G. J. Ritter, *Ind. Eng. Chem.*, 1929, **1**, 52–54.

65 R. Yulina, R. Srie Gustiani, C. Kasipah, M. Danny Sukardan Balai Besar Tekstil, K. Perindustrian and J. Jenderal Ahmad Yani No, *E3S Web Conf.*, 2020, **148**, 02004.

